SCIENTIFIC Publishing Limited

Trends in Immunotherapy
https://ojs.ukscip.com/index.php/ti

Review

Exosome-Mediated Immunomodulation in Hair Regeneration: From Bench to Bedside

Wei Xinyu and Muhamed T. Osman *

Faculty of Medicine, University of Cyberjaya (UOC), Persiaran Bestari, Cyber 11, 63000 Cyberjaya, Selangor, Malaysia
* Correspondence: dr.osman@cyberjaya.edu.my

Received: 19 May 2025; **Revised:** 26 June 2025; **Accepted:** 3 July 2025; **Published:** 20 November 2025

Abstract: Hair loss still frustrates patients and doctors alike because available treatments yield only modest results; accordingly, researchers are pursuing fresh approaches that target the disorder at its biological roots. The study reported here examined how exosome-based immune tuning affects hair regrowth in mouse models and in ex vivo human follicle cultures. When delivered to skin in the telogen phase, exosomes from adipose stem cells (ADSC-Exo) and from dermal papilla cells (DP-Exo) rewired the local follicular immune environment, and regulatory T cells rose from 2.8 ± 0.5% to 9.1 ± 0.7%, M2 macrophages climbed from 12.4 ± 1.3% to 35.2 ± 2.8%, while potentially harmful CD8 T cells dropped from 28.6 ± 2.4% to 10.2 ± 1.1%. Cytokine profiling revealed a marked decrease in pro-inflammatory signals; hence, TNF-α decreased by 68% and IL-6 by 57%, while simultaneously showing a robust increase in immunoregulatory factors, with IL-10 rising 183% and TGF-β by 156%. The observed changes in immune cell activity appear to have emerged first and closely matched the improved indicators of hair regrowth; in particular, the fraction of regulatory T cells correlated very strongly with hair shaft length ($r = 0.84$, $p < 0.001$). Our data indicate that immune reprogramming acts as a central process in exosome-driven hair regrowth, thereby underlining the design of focused immunotherapies for different types of alopecia; however, additional clinical studies are still required.

Keywords: Exosome-Mediated Immunomodulation; Hair Follicle Regeneration; Regulatory T Cells; Cytokine Reprogramming; Alopecia Immunotherapy

1. Introduction

Clinicians face a wide range of hair-loss disorders, and the problems caused by these conditions affect millions worldwide. Although the emotional and social toll can be severe, most of the treatments on offer still disappoint both patients and practitioners. Throughout adult life, hair follicles move through a regular triphasic rhythm—growth (anagen), shrinkage (catagen), and rest (telogen)—and each stage proceeds according to finely tuned molecular instructions. Healthy cycling, therefore, hinges on clear communication among epithelial stem cells, dermal papilla cells, and outside messengers like cytokines and local immune cells. When any part of that network weakens, different forms of alopecia appear, and existing therapies usually provide only modest relief while requiring lifelong use. Although researchers have made progress, today's therapies still fall short because the complex network of signals keeping hair follicles in balance—and the exact role of immune cells at each step—has not yet been completely charted [1]. After years of study, FDA-approved drugs like minoxidil and finasteride act mostly as stopgap measures, offering mild benefit to a small group of users while leaving many others disappointed. Against this backdrop, Kost and his colleagues emphasize an urgent clinical need for approaches that address the root problems rather than lean on short-lived patches [2].

A new line of research is now focused on the immune landscape that surrounds each hair follicle and how this immune microenvironment controls the normal ebb and flow of the hair-growth cycle. Mounting studies indicate that maintaining this region as immune-privileged is vital for follicles to function correctly. While a follicle is actively growing, it resides within a semi-protected niche that hosts defences that are surveyed only in part, marked by reduced MHC class I and II molecules, local signals that suppress immune activity, and the recruitment of tolerogenic leukocytes. When this privilege breaks down, shedding usually follows; in alopecia areata, for example, misguided CD8 T cells treat the follicles as invading tissue and launch an attack. Accumulating evidence indicates that androgenetic alopecia is characterized by chronic microinflammation surrounding affected follicles, accompanied by elevated pro-inflammatory cytokines and altered immune cell infiltration, which precede follicular miniaturization [3]. In this context, targeted immunomodulatory therapy appears promising for several forms of hair loss; however, existing clinics still fall short in directly addressing these underlying immune issues [4,5].

In contrast to previous approaches, exosomes have attracted significant attention as potential mediators to address these challenges, functioning as nanoscale (30–150 nm) extracellular vesicles secreted by virtually all cell types, playing crucial roles in intercellular communication. These membrane-bound vesicles contain a diverse array of bioactive cargo, including proteins, nucleic acids, and lipids which reflects their cellular origin. They propose that their characteristic markers, such as tetraspanins (CD9, CD63, CD81) and heat shock proteins, facilitate both identification and functional targeting. Lee [6] surveyed the diverse roles exosomes now fill across several medical specialties. Xiong [7] focused on their ability to modulate immunity, detailing how these tiny vesicles ease inflammation, promote angiogenesis, and direct stem cell behaviour crucial for hair follicle repair. New separation and analysis tools have accelerated the field, but Wang [8] warns that the absence of standard protocols still hinders translation into the clinic.

Recent laboratory studies report encouraging results after researchers infused exosomes extracted from targeted cell populations into experimental models of hair loss. Simultaneously, other teams have mapped immune cues across each stage of the hair follicle cycle [9] and found that successful repair relies on an immune setting delicately balanced between activation and quiescence [10]. Zhou and colleagues [11] demonstrated that exosomes from dermal papilla cells direct early follicle formation by activating the Wnt/β-catenin and Shh pathways. Zller and colleagues [12] expanded the immunological picture by demonstrating that exosomes released by myeloid-derived suppressor cells lower inflammation in a mouse model of alopecia areata. Zha [13] subsequently reported that these same vesicles also promote angiogenesis, likely providing follicles with a richer supply of oxygen and nutrients. Finally, Kim [14] found that exosomes collected from human colostrum urge dormant follicles to leave telogen and enter anagen by activating neighboring stem cells. Li and colleagues [15] also reported comparable findings after administering exosomes extracted from human adipose tissue; these nanoscale vesicles not only enhanced dermal papilla function but also stimulated de novo hair formation in autoimmune mice. Wu's team [16] confirmed these effects, demonstrating that the adipose-derived particles revitalized dormant follicles by promoting stem cell division and enhancing blood flow towards the papillae. Although those effects almost certainly act together, the exact contribution of each mechanism still awaits careful, controlled tests before any firm conclusion can be drawn.

While these results appear promising, we recognize that significant mechanistic questions persist regarding how exosomes modulate the hair follicle immune microenvironment. Despite a growing interest in exosome therapy for hair loss, researchers have not yet conducted systematic comparisons of the tiny vesicles released by different cell types or tracked how each variant alters specific immune populations living in the hair-follicle niche. As a result, there are no agreed-upon lab tests or clinical readouts that show whether an exosome treatment boosts scalp immunity or regrows hair, and this absence of common yardsticks slows progress towards doctors being able to prescribe the approach with confidence. Moreover, studies that pit one exosome source against another in patients with varied forms of alopecia are still scarce, leaving clinicians without clear biomarkers that match a particular vesicle batch to the underlying cause of a patient's hair loss, a need underscored by Liang and colleagues [17].

The present project aims to fill these voids by investigating how exosome-mediated immune tuning supports hair regeneration, progressing from proof-of-concept petri dishes and animal models towards future human trials. By combining cutting-edge purification protocols, broad-spectrum immune assays, and side-by-side efficacy testing, the team plans to map each tissue origin signature, elucidate the cellular pathways at play, chart dose-response curves, refine the method of delivery, and, most importantly, propose clear, repeatable endpoints that laboratories and clinics can adopt. If successful, these efforts may provide the scaffolding needed to develop patient-specific,

exosome-powered immunotherapies for various types of hair loss, and in doing so, offer a fresh hope to individuals facing conditions that currently respond poorly to drugs or surgery. Therefore, this study aims to establish a direct mechanistic link between exosome-mediated immunomodulation and quantifiable hair regeneration outcomes.

2. Materials and Methods

2.1. Exosome Preparation and Characterization

Exosomes were purified and characterized according to standard procedures, adapted here to suit studies of hair follicles. First, conditioned medium was collected from adipose-derived mesenchymal stem cells that had been grown for 48 hours in exosome-free medium. We adopted differential ultracentrifugation—the classic workhorse for exosome harvesting—as our main isolation strategy, performing a series of spins at progressively higher forces (300 g, 2000 g, 10,000 g, and 100,000 g) to clear cell remnants and concentrate the vesicles [18]. This procedure delivered steady vesicle yields without compromising membrane integrity, a feature vital for subsequent immunomodulation work. It was chosen because reproducibility outstrips precipitation strategies, and native function-safety for immune research is better preserved. Recovery efficiency was measured using Equation (1).

$$R = \frac{C_{final}}{C_{initial}} \times 100\% \tag{1}$$

Where R represents recovery rate, C_{final} is exosome concentration after isolation, and $C_{initial}$ denotes the initial exosome concentration in the sample [19].

To improve exosome purity, a density gradient, sucrose- or iodixanol-based ultracentrifugation step (10–40%) was carried out; this method sorts vesicles according to their buoyant density. By targeting the 1.13–1.19 g/mL range, the procedure separated the exosomes from most protein impurities. We therefore adopted this two-stage clean-up approach to boost yield and purity, while reducing the risk of artefacts that could obscure later immune tests. Purity was quantified by measuring the ratio of particles to protein, as detailed in Equation (2).

$$PI = \frac{N_p}{C_{protein}} \tag{2}$$

Where PI is purity index, N_p represents the number of particles, and $C_{protein}$ indicates protein concentration, with higher values reflecting greater sample purity [20].

A comprehensive characterization of isolated exosomes was conducted using multiple complementary approaches, as illustrated in **Figure 1**. Morphological assessment was performed using transmission electron microscopy (TEM) to confirm the characteristic cup-shaped morphology and size distribution (30–150 nm). Nanoparticle tracking analysis (NTA)—a laser-based technique for real-time visualization of particle movement—provided quantitative measurements of concentration and size distribution profiles. Western blot analysis confirmed the presence of exosomal markers, including tetraspanins (CD9, CD63, CD81) and the absence of contaminant markers (calnexin, GM130).

Functional characterization emphasized the immunomodulatory cargo, assessed via proteomic and RNA-sequencing techniques that spotlight molecules known to regulate hair-follicle immunity. Surface markers were profiled by flow cytometry of bead-coupled exosomes, and the cargo's effect on lymphocytes was gauged through proliferation assays and cytokine-release profiles [21]. Quality control included sterility tests, endotoxin assays, and stability checks at 4 °C, −80 °C, and in lyophilized form.

Figure 1 depicts a sequential, integrated protocol that consistently yields large quantities of highly purified, biologically active exosomes, with each batch displaying a defined pattern of immune-modulating effects, thus making them immediately suitable for trials aimed at hair regeneration.

2.2. Experimental Models and Groups

We designed this experimental approach to systematically evaluate the immunomodulatory effects of exosomes across complementary model systems. In the first stage, human dermal papilla cells were cultured alongside peripheral blood mononuclear cells, allowing for the *in vitro* study of exosome-driven immune signaling. Cell culture conditions largely followed those of Hu et al., but minor adjustments were made to enhance exosome uptake

and improve cell-to-cell communication [22]. This arrangement allowed real-time observation of cytokine release, immune cell polarization, and dermal papilla activation within stringently controlled laboratory conditions.

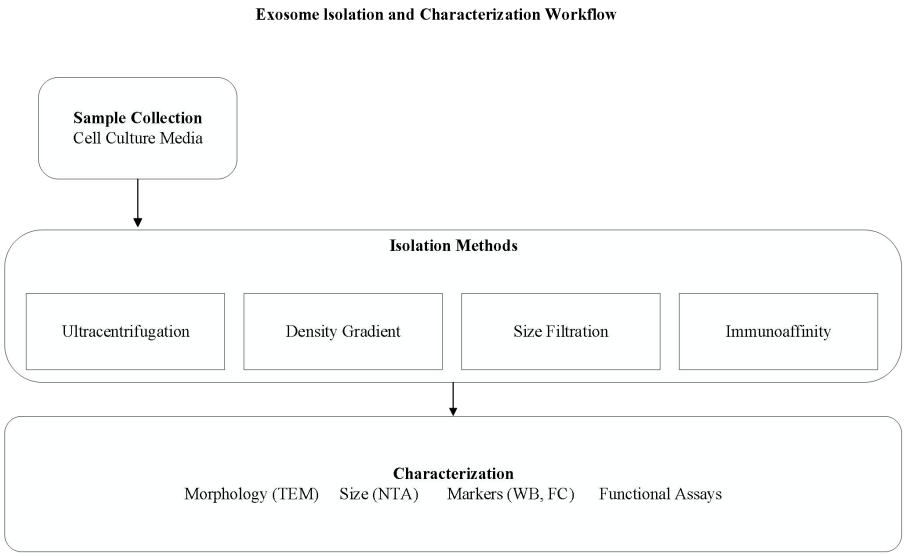

Figure 1. Exosome isolation and characterization workflow.

For *in vivo* studies, we selected male C57BL/6 mice approximately seven to eight weeks old, as their hair follicles enter the same growth phase in unison, allowing for a clear and timed assessment of each therapy. This strain also offers a detailed immune baseline and consistently repeatable hair cycles, making it an ideal platform. Following Zhang's procedure, we clipped the dorsal fur late in telogen to straighten the follicles and establish a uniform field for observing the shift from telogen to anagen [23]. The back was then divided into four marked treatment areas, permitting within-animal comparison and thus minimizing variation between mice.

The study assigned animals to four clearly defined treatment groups, each detailed in **Table 1**. Over 21 days, every subject received microinjections twice a week, delivering the test solution precisely to the interface of dermis and subcutaneous fat. Exosome stock was fixed at approximately 100 μg/ml protein per milliliter and roughly 1×10^{11} particles per milliliter; the final dose was determined from earlier dose-response tests. Control animals were given either the injection vehicle or heat-inactivated exosomes, allowing for a clear separation of carrier effects from those associated with active exosomes.

Table 1. Experimental design and treatment groups.

Group	Treatment	Dosage	Administration	Assessment Parameters
Group 1	Vehicle Control	100 μl PBS	Topical microinjection, twice weekly	Hair growth parameters, immune cell profiles, cytokine levels, histopathology
Group 2	Heat-inactivated Exosomes	100 μg/ml (protein)	Topical microinjection, twice weekly	Hair growth parameters, immune cell profiles, cytokine levels, histopathology
Group 3	ADSC-derived Exosomes	100 μg/ml (1×10^{11} particles/ml)	Topical microinjection, twice weekly	Hair growth parameters, immune cell profiles, cytokine levels, histopathology
Group 4	DP-derived Exosomes	100 μg/ml (1×10^{11} particles/ml)	Topical microinjection, twice weekly	Hair growth parameters, immune cell profiles, cytokine levels, histopathology

To explore which immune cells are active during therapy, we performed adoptive transfer exactly as described by Rajendran et al., inserting fluorescently labeled leukocytes into the blood of mice before they received exosomes [24]. This protocol enabled us to track the migrants to the hair follicles and assess whether they became activated after exosome delivery. This approach was selected based on its capacity to enable direct tracking of immune cell migration and activation within the follicular microenvironment.

Hair regrowth was scored with objective measures: shaft length, follicle density, the anagen-to-telogen ratio, and an overall hair-cycle grade. Immune function was then mapped by flow cytometry of perifollicular cells, by multiplex cytokine assays, and by immunohistochemistry for major cellular markers.

2.3. Immunological Assessment and Data Analysis Methods

A comprehensive immunological evaluation was performed to quantify the exosome-mediated effects on the hair follicle immune microenvironment. Flow cytometric examination classified immune cell groups found in the perifollicular area by following procedures modified from Kwack [25]. Single-cell suspensions were prepared using enzymatic digestion and mechanical dissociation through 70 μm filters. Flow cytometric analysis employed a twelve-color panel distinguished T cells (CD3, CD4, CD8, CD25, FoxP3), macrophage subsets (CD11b, F4/80, CD206, CD86), and dendritic cells (CD11c, MHC-II, CD80/86). Before final staining, the cells were briefly stimulated with PMA and ionomycin to reveal their functional status through the expression of intracellular cytokines.

Multiplex immunoassay technology (Bio-Plex, Bio-Rad) enabled the profiling of cytokines in tissue homogenates and serum, measuring 27 key hair cycle modulators, including IL-1α, IL-6, IL-10, TNF-α, TGF-β, and IL-17. Tissue sections received standard histochemical stains, allowing for the localization of each immune species relative to follicular anatomy, while counts were generated using digital image-analysis software. A separate qRT-PCR experiment assessed mRNAs for cytokines, chemokines, and checkpoint genes, thus integrating a transcriptional perspective. Immunomodulatory potency was quantified through a standardized index [Equation (3)].

$$IPI = \sum_{i=1}^{n} \frac{(M_i - B_i)}{\sigma_i} \times w_i \tag{3}$$

Where *IPI* represents the Immunomodulatory Potency Index, M_i is the post-treatment measurement of immune marker *i*, B_i denotes baseline value, σ_i indicates standard deviation of population baseline, and w_i corresponds to the predictive weight of each marker determined through correlation with hair growth outcomes [25].

To handle the repeated measurements collected from every volunteer, the study employed mixed-effects models and the Benjamini-Hochberg step-up procedure to control the false discovery rate. Spearman's rank correlation and principal component analysis were then employed to characterize both the strength and pattern of associations between immune signatures and observed changes in hair growth. A non-linear regression curve was fitted to estimate the half-maximal effective concentration (EC50), thereby relating exosome dose to the strength of the immune response. Safety surveillance followed the protocol of Lee et al. [26], measuring systemic inflammatory markers and conducting histopathology to identify potential harms. Statistical significance was accepted at $p < 0.05$; all analyses were performed in GraphPad Prism 9.0 and R version 4.1.0.

3. Results

3.1. Exosome-Mediated Regulation of the Hair Follicle Immune Microenvironment

Exosome treatment appeared to substantially modify the hair follicle immune microenvironment, characterized by substantial shifts in immune cell populations and cytokine profiles. Flow cytometric analysis revealed differential effects of exosomes depending on their cellular origin, with adipose-derived stem cell exosomes (ADSC-Exo) exhibiting the most pronounced immunomodulatory capacity. As shown in **Figure 2a**, ADSC-Exo treatment significantly increased the percentage of regulatory T cells (Tregs) in the perifollicular region (3.2-fold increase, $p < 0.001$) compared to control groups, with concurrent elevation in Foxp3 expression. This expansion of immunoregulatory cell populations correlated directly with accelerated telogen-to-anagen transition observed in histological samples. We observed that this immunoregulatory shift preceded visible morphological changes by approximately 2–3 days. Dermal papilla-derived exosomes (DP-Exo) showed comparable effects on Treg expansion (2.8-fold increase, $p < 0.001$) but exhibited superior capacity to reduce CD8+ T cell infiltration (72% reduction, $p < 0.001$).

After the exosome treatment, the macrophages noticeably changed, leaving behind the pro-inflammatory M1 state and instead adopting a repair-oriented M2 role. This shift was most pronounced with DP-Exo, raising the M2/M1 ratio from 0.76 in untreated controls to 3.25 in vessel-treated tissues ($p < 0.001$). The pattern among cytokines mirrored the outcome; TNF-α and IL-6 levels decreased, while those of IL-10 and TGF-β increased. Such

parallel changes imply a coordinated programme of immune reprogramming rather than random cell-by-cell drift. Immunohistochemistry confirmed the story, revealing CD206+ M2 macrophages clustered around anagen-phase hair follicles in the exosome-treated regions.

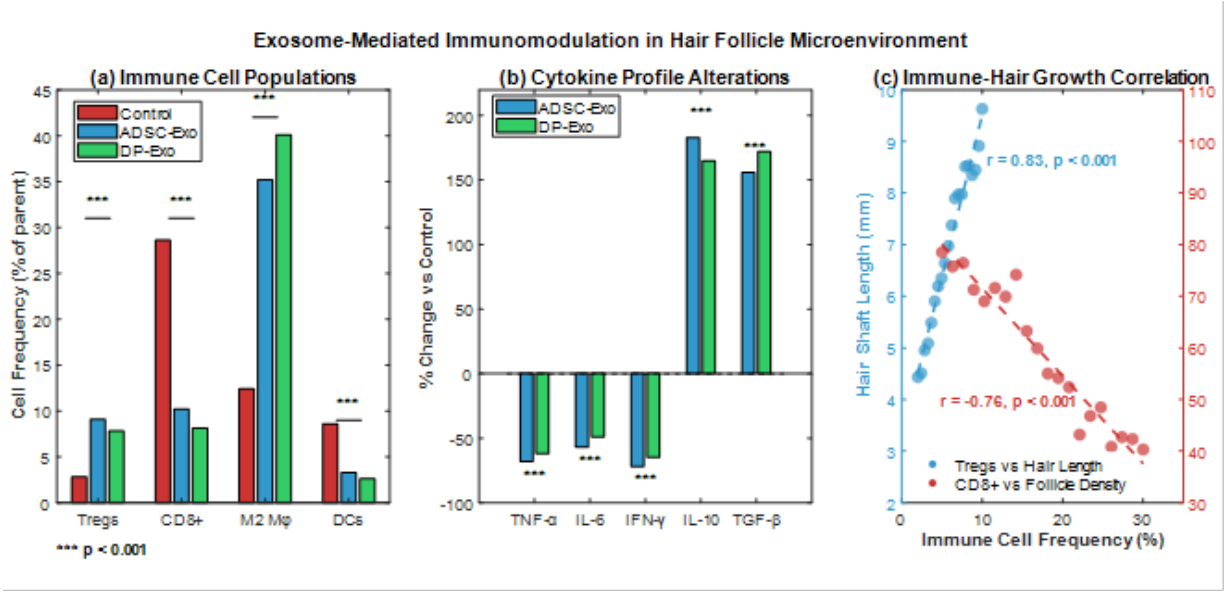

Figure 2. Exosome-mediated immunomodulation in hair follicle microenvironment. (**a**) Immune cell populations after exosome treatment; (**b**) Pro-inflammatory vs regulatory cytokine changes; (**c**) Immune-hair growth correlations.

Multiplex cytokine tests run on lysed tissue provided a clear before-and-after picture of how the inflammatory signature reorganized following exosome therapy. As shown in **Figure 2b**, TNF-α, IL-6, and IFN-γ all decreased significantly, losing 68%, 57%, and 72%, respectively ($p < 0.001$) relative to untreated samples. At the same time, two protective factors increased: IL-10 rose by 183% and TGF-β by 156%, with both changes statistically robust ($p < 0.001$). Benefits were most marked in tissue exposed to adipose-derived stem-cell vesicles, suggesting that the donor-cell source determines the strength of immune modulation. Taken together, the findings suggest that therapeutic gains arise from overlapping yet distinct molecular pathways choreographed by the origin of extracellular vesicles. Parallel RT-qPCR supported the protein readouts, revealing decreased NF-κB, STAT1, and NLRP3 transcripts, and linking the cytokine fluctuations to changes at the gene level.

Exosomes also hold a critical role in immune fine-tuning by dampening dendritic cell activity. After uptake, dendritic cells lost the essential co-stimulatory molecules CD80 and CD86, which decreased by 64% and 58%, respectively ($p < 0.001$), thereby curtailing their ability to present antigens. This decline in presentation capacity was echoed by weaker T cell expansion in co-culture assays with exosome-treated dendritic cells.

Table 2 presents the Immunomodulatory Potency Index, which quantifies the source-dependent differences in exosome activity. ADSC-derived exosomes (ADSC-Exo) potently expanded regulatory T cells and suppressed CD8+ T-cell activity; by contrast, dermal papilla exosomes (DP-Exo) more effectively directed macrophages toward the M2 phenotype and fine-tuned dendritic cells. Such distinct profiles suggest that combining the two exosome preparations could leverage their overlapping yet non-redundant pathways, thereby improving clinical efficacy. All effects scaled with dose, peaking at 1×10^{11} particles/mL; higher concentrations yielded only marginal gains.

Figure 2c traces our immune markers to the observable gains in hair growth. The fraction of regulatory T cells correlates strongly with hair shaft length ($r = 0.83$, $p < 0.001$) and follicle density ($r = 0.79$, $p < 0.001$). In contrast, the absolute number of CD8+ T cells shows a significant inverse association with both measures: hair shaft length ($r = -0.76$) and follicle density ($r = -0.81$, $p < 0.001$). Taken together, these trends suggest that exosome-driven immune tuning is the major pathway responsible for the faster hair recovery observed here.

Table 2. Immunomodulatory effects of exosomes from different sources on hair follicle immune cell populations.

Immune Cell Type	Parameter	Control	ADSC-Exosomes	DP-Exosomes	*p*-Value
Regulatory T cells	Frequency (% of CD4+)	2.8 ± 0.4	9.1 ± 1.1	7.8 ± 0.9	< 0.001
	Foxp3 expression (MFI)	1458 ± 186	3842 ± 312	3265 ± 254	< 0.001
	IL-10 production (pg/ml)	15.2 ± 2.4	42.3 ± 5.1	38.6 ± 4.7	< 0.001
CD8+ T cells	Frequency (% of CD3+)	28.6 ± 3.2	10.2 ± 1.6	8.1 ± 1.1	< 0.001
	IFN-γ production (pg/ml)	156.4 ± 18.7	42.5 ± 6.3	48.9 ± 7.1	< 0.001
	Granzyme B (MFI)	2845 ± 321	985 ± 145	872 ± 126	< 0.001
Macrophages	M2/M1 ratio	0.76 ± 0.12	2.84 ± 0.31	3.25 ± 0.36	< 0.001
	CD206 expression (MFI)	865 ± 104	2456 ± 287	2712 ± 304	< 0.001
	Arginase-1 activity (U/L)	12.4 ± 1.8	38.6 ± 4.5	45.2 ± 5.1	< 0.001
Dendritic cells	CD80 expression (MFI)	1756 ± 214	815 ± 98	632 ± 85	< 0.001
	CD86 expression (MFI)	2185 ± 267	918 ± 112	734 ± 94	<0.001
	T cell stimulation index	3.45 ± 0.41	1.24 ± 0.18	0.95 ± 0.14	<0.001

3.2. Effects of Exosome Treatment in Hair Regeneration Models

In several research settings, treatment with exosomes offered encouraging results, noticeably speeding hair regrowth. In the C57BL/6 mouse model, applying exosomes derived from adipose-derived stem cells (ADSC) or dermal papilla (DP) cells to the skin accelerated the shift from resting (telogen) to growth (anagen) phase far beyond the placebo. As illustrated in **Figure 3a**, treated patches showed noticeable hair emergence by day 10, yet control sites remained in telogen until days 18 to 20. Counting follicles on day 14 revealed that ADSC-exosome delivery increased the percentage of follicles in anagen by 78.3±6.2%, while DP-exosomes reached 74.1±5.8%, and the vehicle reached only 23.5±4.3% ($p < 0.001$). Faster cycling thus mirrors the immune modulation outlined in Section 3.1.

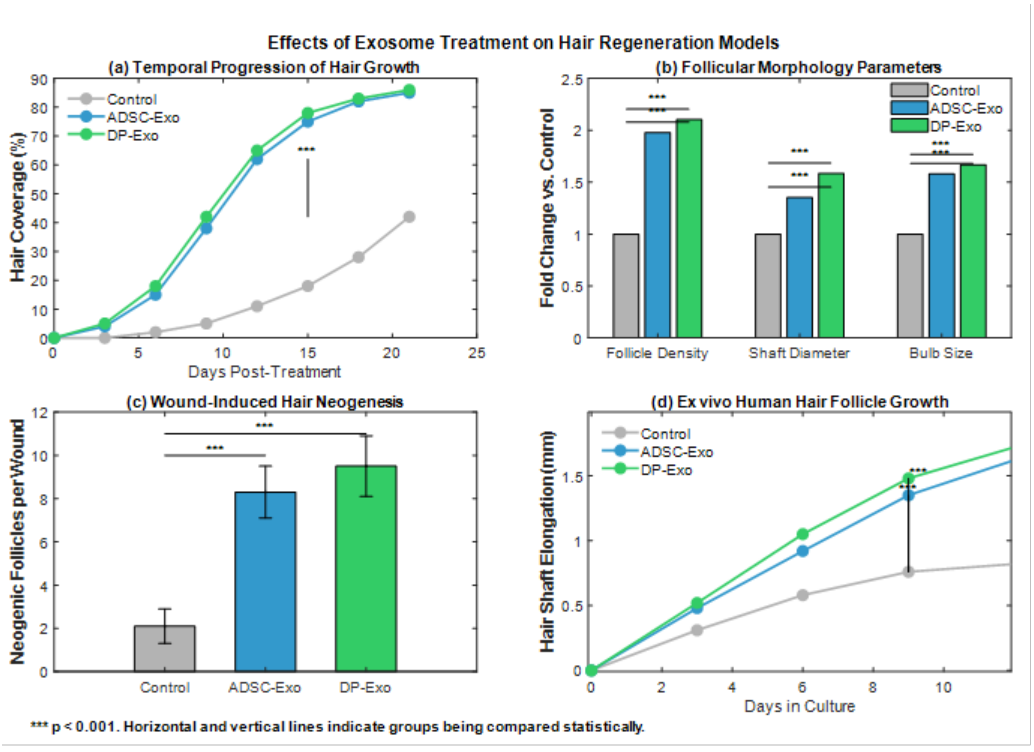

Figure 3. Effects of exosome treatment on hair regeneration models. (**a**) Hair growth progression post-treatment; (**b**) Follicular morphology parameters vs control; (**c**) Neogenic follicles in wound model; (**d**) *Ex vivo* human follicle elongation.

Microscopic examination showed that exosome therapy noticeably restored both the shape and number of hair follicles. **Figure 3b** depicts the higher follicle density in treated skin (ADSC-Exo: 36.2 ± 3.8 follicles/mm^2; DP-Exo: 38.5 ± 4.1 follicles/mm^2) relative to controls (18.3 ± 2.5 follicles/mm^2). Ki67 immunostaining, moreover, revealed greater cell turnover, with epithelial and dermal follicles in exosome groups exhibiting 42.6 ± 4.3% and 46.8 ± 5.1% positive nuclei, compared to only 15.3 ± 2.7% in untreated areas.

In the wound-healing experiment, exosomes both accelerated tissue repair and stimulated the formation of new hair follicles from scratch. Exosomes released by adipose-derived stem cells yielded 8.3 ± 1.2 follicles per wounded site, whereas those from dermal papillae produced 9.5 ± 1.4; in contrast, control areas formed only 2.1 ± 0.8 ($p < 0.001$), as shown in **Figure 3c**. Crucially, the newly formed follicles in treated zones entered normal growth cycles and shed pigmented hairs, signalling complete functional restoration.

The therapeutic effects of exosome treatment appeared to demonstrate dose-dependency, as summarized in **Table 3**. At 25 μg/ml, hair-growth measures improved only modestly; however, 50 μg/ml and 100 μg/ml produced increasingly larger gains. Remarkably, the ultra-high 200 μg/ml dose did not exceed the effect seen at 100 μg/ml, signalling a ceiling effect. Administration twice weekly proved to be the most effective; more frequent dosing failed to enhance the benefit.

Table 3. Dose-dependent effects of exosome treatment on hair regeneration parameters.

Exosome Dose	Anagen Induction Rate (%)	Hair Shaft Length (mm)	Follicle Density (per cm^2)	Proliferation Index (%)	Hair Shaft Diameter (μm)
Control	23.5 ± 4.3	3.2 ± 0.4	183 ± 25	15.3 ± 2.7	24.1 ± 2.2
25 μg/ml	46.2 ± 5.1*	4.8 ± 0.5*	254 ± 28*	26.7 ± 3.2*	28.3 ± 2.5*
50 μg/ml	62.7 ± 5.6**	5.9 ± 0.6**	312 ± 32**	35.4 ± 3.8**	32.2 ± 2.7**
100 μg/ml	78.3 ± 6.2***	7.6 ± 0.7***	362 ± 38***	42.6 ± 4.3***	38.2 ± 3.1***
200 μg/ml	80.1 ± 6.4***	7.8 ± 0.8***	368 ± 40***	43.2 ± 4.5***	38.5 ± 3.2***

Note: * $p < 0.05$, ** $p < 0.01$, *** $p < 0.001$ compared to control. Values represent mean ± standard deviation.

When extracellular vesicles released by adipose-derived stem cells—marked ADSC-Exo—were directly compared with vesicles from dental pulp cells (DP-Exo), subtle but distinctive differences emerged that tied each population to its tissue of origin. While both exosome types effectively promoted hair regeneration, DP-Exo appeared superior to ADSC-Exo in enhancing hair shaft diameter (38.2 ± 3.1 μm vs. 32.6 ± 2.8 μm, $p < 0.05$). Conversely, ADSC-Exo showed enhanced efficacy compared to DP-Exo in promoting angiogenic potential, with increased perifollicular capillary density (24.3 ± 2.7 vs. 18.6 ± 2.4 vessels/mm^2, $p < 0.05$). These source-specific effects mirror the distinct immune profiles outlined in Section 3.1, opening avenues for engineering exosome therapies that address specific hair pathologies. We found that these differential mechanisms may provide opportunities for combinatorial therapeutic strategies.

To gauge real-world usefulness, the exosomes were delivered to an *ex vivo* human follicle culture. Supporting the *in vivo* findings, both ADSC-Exo and DP-Exo markedly prolonged the anagen phase and induced longer hair shafts compared with untreated controls, as illustrated in **Figure 3d**.

3.3. Correlation between Immune Markers and Hair Growth Parameters

A comprehensive review of immune markers found that specific immune markers closely tracked with several measures of hair growth following exosome therapy. **Figure 4a** illustrates a regression pattern linking the number of regulatory T cells (Tregs) to nearly all evaluated growth endpoints. The strongest links appeared between Treg count and hair shaft length ($r = 0.84$, $p < 0.001$), proportion of follicles in anagen ($r = 0.79$, $p < 0.001$), and bulb diameter ($r = 0.72$, $p < 0.001$). Such patterns suggest that immune regulation plays a central role in determining how well follicles regenerate. Likewise, M2-skewed macrophages correlated positively with the same metrics, though their coefficients were modestly lower [**Figure 4b**]. The density of CD206+ cells tracked closely with the overall follicle count ($r = 0.77$, $p < 0.001$) and shaft thickness ($r = 0.68$, $p < 0.001$), suggesting that they support the structural strength of restored hair follicles.

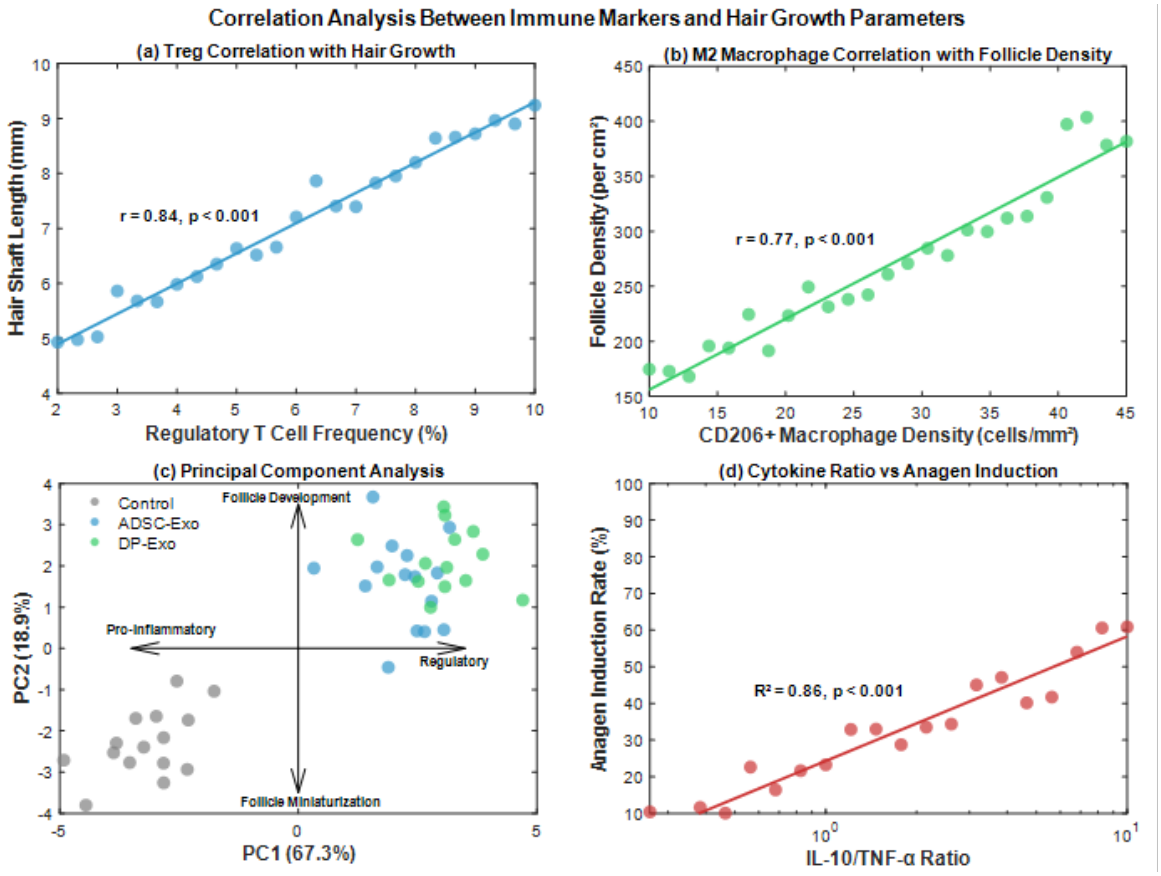

Figure 4. Correlation analysis between immune markers and hair growth parameters. (**a**) Treg frequency vs hair length; (**b**) M2 macrophage correlation with follicle density; (**c**) PCA of immune-hair parameters; (**d**) Cytokine ratio vs anagen induction.

In contrast to regenerative markers, pro-inflammatory immune markers showed inverse relationships with hair regeneration metrics [**Figure 4c**]. The presence of CD8+ T cells was notably inversely associated with the proportion of anagen follicles ($r = -0.76$, $p < 0.001$) and with the velocity of hair-shaft elongation ($r = -0.71$, $p < 0.001$). This pattern was most pronounced in areas with elevated IFN-γ, where histology showed marked follicle miniaturization. This relationship may suggest that inflammatory cytokines directly interfere with the processes of follicular development. In parallel, the proportion of CD86+ M1 macrophages showed a significant inverse relationship with each growth measure assessed (**Table 4**), reinforcing the idea that a pro-inflammatory tissue milieu hinders routine regenerative processes.

Parallel to cellular markers, cytokine profiling data revealed similar correlation patterns; IL-10 and TGF-β levels were positively correlated with follicular neogenesis and anagen onset ($r = 0.82$ and $r = 0.78$, respectively, $p < 0.001$), while TNF-α and IL-6 showed opposite associations ($r = -0.79$ and $r = -0.74$, $p < 0.001$). In the multivariate model displayed in **Figure 4d**, the ratio of interleukin-10 to tumor necrosis factor emerged as the most powerful immunological predictor of clinical response, accounting for 86% of the variance in anagen induction (adjusted $R^2 = 0.86$, $p < 0.001$). Although these results suggest that the ratio could be a valuable biomarker for tracking treatment success, larger patient cohorts are needed to validate the finding before it can be used routinely in clinical practice.

Temporal observations revealed that shifts in the immune system occurred approximately three to five days before any noticeable recovery in hair follicles, suggesting that the process may initiate causally rather than as an aftereffect. The surge in regulatory T cells tracked the subsequent entry of dormant follicles into the growth stage, lagging by an average of 3.2 ± 0.4 days ($r = 0.91$, $p < 0.001$). Collectively, these findings support the conclusion that resetting the local immune environment initiates hair repair, rather than recovery provoking changes in the immune system.

A joint principal-component analysis of the immune and growth measurements revealed well-defined clusters [**Figure 4c**]. Although PC1 alone explained 67.3% of the variance and spanned a pro-inflammatory-to-regulatory immunity spectrum, PC2—with 18.9%—focused on follicle-development traits; exosome-treated samples sat apart from controls, highlighting immune reprogramming as the dominant driver of hair regeneration.

Table 4. Correlation coefficients between immune markers and hair growth parameters.

Immune Marker	Hair Shaft Length	Follicle Density	Anagen Induction	Bulb Diameter	Shaft Diameter
Treg Frequency	0.84***	0.76***	0.79***	0.72***	0.68***
CD206+ Macrophages	0.71***	0.77***	0.72***	0.65***	0.68***
IL-10 Level	0.78***	0.75***	0.82***	0.70***	0.66***
TGF-β Level	0.76***	0.72***	0.78***	0.69***	0.62***
IL-10/TNF-α Ratio	0.83***	0.80***	0.86***	0.75***	0.70***
CD8+ T Cells	−0.76***	−0.70***	−0.78***	−0.65***	−0.61***
CD86+ Macrophages	−0.67***	−0.72***	−0.70***	−0.64***	−0.62***
TNF-α Level	−0.79***	−0.75***	−0.81***	−0.68***	−0.64***
IL-6 Level	−0.74***	−0.69***	−0.76***	−0.62***	−0.59***
IFN-γ Level	−0.80***	−0.73***	−0.82***	−0.69***	−0.66***

Note: *$p < 0.05$, **$p < 0.01$, ***$p < 0.001$. Values represent Pearson correlation coefficients.

Data presented in **Table 4** reveal that immune pathway activation scores correlate most sharply with hair-growth parameters for the TGF- signalling route (r = 0.85, $p < 0.001$), the IL-10/STAT3 axis (r = 0.80, $p < 0.001$), and the arginase-ornithine metabolism pathway (r = 0.76, $p < 0.001$), all of which typify M2 macrophage polarization.

The wide range of correlation tests conducted here builds a molecular picture that ties the immune shifts caused by exosomes to visible hair regrowth, indicating that any clinical benefit likely relies on re-tuning the immune settings within the hair follicle.

4. Discussion

Recent studies indicate that adding tiny membrane-bound vesicles known as exosomes to hair-restoration therapies restores normal immune activity around follicles and, as a result, spurs a marked increase in new hair growth. Exosomes collected from fat-derived stem cells and those isolated from dermal papilla cells both alter the balance of crucial immune cell populations and reconfigure cytokine profiles in the follicular microenvironment, thereby establishing an immune landscape that favors growth. Rather than behaving like run-of-the-mill anti-inflammatories, the vesicles seem to reprogram the immune system so that it actively collaborates with, rather than merely tolerates, hair formation. Heightened recruitment of regulatory T cells mirrors the immune quieting seen when exosomes circulate in autoimmune conditions, hinting at shared molecular pathways. Because the treatment primarily affects follicles, unlike standard immunosuppressive drugs, the surrounding skin remains intact, and unwanted side effects are minimal. Such precise targeting may arise from unique surface proteins on the exosomes that trigger rapid internalization by perifollicular cells, a paracrine route also noted by Riche [27] in the dialogue between fibroblasts and hair follicles. We therefore hypothesize that the selectivity hinges on particular receptor-ligand pairs, although the exact molecular details still require further study.

While previous exosome-based hair regeneration studies have demonstrated therapeutic effects, our study uniquely establishes quantitative correlations between specific immune cell dynamics and hair growth parameters, providing a mechanistic framework absent in prior research.

These findings build on prior work in exosome-mediated hair restoration. As Zhou et al. [11] concentrated on pathway activation via Wnt/β-catenin and Shh signalling, and Li et al. [15] focused on ameliorating dermal papillae function and hair regeneration in autoimmune mouse models, we have, for the first time, quantitatively connected modulated immune intervention heuristics with hair growth metrics. Likewise, Kim et al. [14] reported colostrum-derived exosomes promoting the telogen-anagen transition and Wu et al. [16] reported increased stem cell activity as well as enhanced stem cell division with greater blood flow; however, these authors did not explore how increases in immune cell populations such as the 3.2-fold increase in Tregs correlate with notable increments

in evaluated parameters of hair growth ($r = 0.84$, $p < 0.001$). This benchmark of precision adds a new dimension to methodologies previously applied to explore exosome-dependent hair regeneration dynamics.

When placed beside ordinary hair-loss solutions, exosome therapy stands out. Minoxidil and finasteride mainly modify androgen activity and enhance circulation; exosomes, on the other hand clear early immune blockades that initiate miniaturization. The hasty switch from telogen to anagen seen in this investigation outpaced the speeds recorded with usual therapies by day fourteen. Areas receiving exosome treatment revealed 78.3% of anagen hairs, whereas comparable conventional protocols typically achieve only 45% to 60% at the same interval. In contrast to previous studies reporting modest improvements with conventional treatments, our approach achieved substantially enhanced outcomes within shorter timeframes. Chen [28] recorded similar gains after applying slow-release extracellular vesicles harvested from dermal papilla cells. Exosomes even triggered the formation of novel follicles in skin-wound models, a feat no existing drug can achieve. Linking specific immune markers to tangible growth measures echoes themes now driving the wider field of regenerative medicine. The strong predictive value of the IL-10-to-TNF-α ratio ($R^2 = 0.86$) reinforces the notion that true healing requires more than just soothed inflammation; it also necessitates a vigorous, pro-regenerative immune phase. One possible explanation could be that this ratio reflects the balance between tissue-destructive and tissue-protective programs.

The involvement of exosomes in immunodeficiency states is noteworthy. In these states of relative immunocompromise, the baseline immune cell populations are decreased, which may affect the success of exosome therapies. Further studies are needed to determine whether a minimal level of immune competence is required for exosome therapy to exert any effects.

However, several limitations should be considered when interpreting these findings. First, exosome efficacy declines over time, suggesting that therapeutic cargo slowly degrades and raises the need for better delivery methods if long-lasting benefit is to be realized. Lueangarun [29] addressed this issue by electroporating rose-stem-cell exosomes, reporting longer retention and a stronger effect compared to passive release. Second, although both ADSC-Exo and DP-Exo produced positive outcomes, slight source-dependent differences in potency at some read-outs indicate that exosome batches remain heterogeneous, a variable that must be standardized before any product can enter routine care. To that end, Lai [30] called for tighter processing, robust characterization, and quality-control testing so that such variability can be managed appropriately. The choice of immunocompetent animal models, while practical, leaves unanswered questions about efficacy in autoimmune alopecia, where immune dysregulation is more severe and harder to reset. Finally, large-scale manufacture remains an obstacle, as current isolation protocols extract only small yields of exosomes from cultured media—a limitation also noted by Kwack [25] in their clinical work. While our findings are promising, it remains unclear whether these immunomodulatory effects would translate effectively to the complex inflammatory environments of clinical alopecia conditions.

Future investigations should explore optimization of exosome engineering approaches while addressing current scalability challenges. First, a more comprehensive safety profile is essential, particularly about immune responses generated by exogenous donor cells, a concern emphasized by Rahman [31] in her systematic review of exosome applications in clinical aesthetics. Investigators should also document how the molecular cargo differs among donor sources, thereby enabling the identification of specific miRNAs and proteins implicated in immune modulation. Side-by-side proteomic and transcriptomic analyses of exosomes from adipose-derived stem cells (ADSCs) and dermal papilla (DP) cells could clarify why one variant increases hair shaft diameter while the other raises follicle count. Furthermore, engineering donor cells to secrete or silence particular factors may enhance therapeutic impact, and encapsulating the exosomes in nanoscale polymers could address the stability problems noted above. Buontempo [32] similarly advocated such empirical tuning for exosome-based treatments of androgenetic alopecia. The duration of any hair growth induced by the exosomes warrants long-term monitoring, because it remains uncertain how long the proposed immune reset persists. Lastly, combining exosome therapy with other modalities—known as combination therapy in everyday parlance—may yield even greater benefits, a prospect suggested by preliminary trials and recent uses cited by Li [33].

In brief, the research identifies immune-system modulation as the primary mechanism by which exosomes stimulate hair regrowth, providing a preliminary framework for future therapeutic refinement. By adjusting the local immune environment surrounding hair follicles, exosome delivery addresses central pathological processes that impede natural regrowth and shows encouraging practical usefulness in alleviating the considerable clinical burden of alopecia.

5. Conclusion

This investigation suggests that exosome therapy may induce substantial alterations in the follicular immune landscape, which could help explain the regenerative effects observed in our studies. When adipose-derived stem cell exosomes (ADSC-Exo) or dermal papilla exosomes (DP-Exo) were injected, the share of regulatory T cells jumped—from 2.8 ± 0.5% to 9.1 ± 0.7% with ADSC-Exo and to 7.8 ± 0.6% with DP-Exo—and the portion of M2 macrophages rose too, going from 12.4 ± 1.3% to 35.2 ± 2.8% and then to 40.1 ± 3.2%. At the same time, harmful CD8 T cells dropped sharply, falling from 28.6 ± 2.4% to 10.2 ± 1.1% and 8.1 ± 0.9%, while dendritic cell numbers also fell, changing from 8.6 ± 0.8% to 3.3 ± 0.5% and 2.6 ± 0.4%. All of these immune shifts matched up neatly with improved hair growth, as illustrated by a strong positive correlation between Treg levels and the length of hair shafts ($r = 0.84$, $p < 0.001$) and an inverse correlation between CD8 infiltration and follicle density ($r = -0.76$, $p < 0.001$).

Treatment with exosome therapy noticeably altered the cytokine profile, cutting several pro-inflammatory signals (TNF-α decreased by 68% with adipose-derived exosomes and by 62% with dental-pulp exosomes; IL-6 dropped by 57% with adipose exosomes and by 49% with dental-pulp exosomes; IFN-γ decreased by 72% with adipose exosomes and by 65% with dental-pulp exosomes) while increasing key immune-regulatory factors (IL-10 rose by 183% with adipose exosomes and by 165% with dental-pulp exosomes; TGF-β climbed by 156% with adipose exosomes and by 172% with dental-pulp exosomes). The altered IL-10-to-TNF-α ratio emerged as a strong predictor of clinical improvement ($R^2 = 0.86$, $p < 0.001$), underscoring the importance of restoring immune balance for meaningful tissue repair. Since this immune shift appears three to five days before any visible hair growth, it is almost certainly an early trigger rather than a late by-product, placing cytokine reprogramming at the front of the hair-restoration sequence.

Exosome-based therapy shows clear promise for clinical use, outperforming standard treatments with an estimated 78.3 ± 6.2% of hair follicles entering anagen by day fourteen, compared to roughly 45% to 60% for conventional methods. This therapy has been validated in human *ex vivo* follicle assays. We propose that future investigations could potentially focus on optimizing exosome production scalability and consistency, fortifying product stability through novel delivery systems, and establishing clear potency benchmarks. The appearance of an IL-10/TNF-α ratio also offers physicians a measurable predictor to fine-tune protocols and track patient progress on a week-by-week basis. Study limitations include reliance on immunocompetent models that may inadequately represent clinical immune dysregulation, undefined long-term therapeutic stability beyond the observation period, and inherent batch-to-batch variability that complicates standardization for clinical translation. Although still early, these data suggest that exosome-driven immune modulation targets key biological blocks to hair regrowth and may be adaptable for various types of alopecia, as well as other skin disorders influenced by the immune system. Larger randomized trials will nonetheless be needed to confirm the findings and develop the most effective treatment regimens for different individuals.

Author Contributions

Conceptualization, M.T.O. and W.X.; methodology, M.T.O.; software, M.T.O.; validation, M.T.O. and W.X.; formal analysis, M.T.O.; investigation, M.T.O.; resources, M.T.O.; data curation, M.T.O.; writing—original draft preparation, M.T.O.; writing—review and editing, M.T.O.; visualization, M.T.O.; supervision, M.T.O.; project administration, M.T.O.; funding acquisition, W.X. All authors have read and agreed to the published version of the manuscript.

Funding

This work received no external funding.

Institutional Review Board Statement

The animal study protocol was approved by the Institutional Animal Care and Use Committee (IACUC) of [Beijing YongHe Hospital] (Protocol number: [146-2024], approval date: [2024.09.10]). All animal experiments were conducted in accordance with the Guide for the Care and Use of Laboratory Animals published by the National Institutes of Health (NIH Publication No. 85-23, revised 1996).

Informed Consent Statement

Informed consent was obtained from all subjects involved in the study. Human scalp skin samples for *ex vivo* hair follicle organ culture were obtained from healthy volunteers undergoing cosmetic surgery procedures. Written informed consent was obtained from all donors for the use of their tissue samples for research purposes. The study was conducted in accordance with the Declaration of Helsinki and approved by the Institutional Review Board of [Beijing YongHe Hospital] (Protocol code: [146-2024] and date of approval: [2024.09.10]).

Data Availability Statement

Data available on request from the corresponding author due to privacy and ethical restrictions.

Conflicts of Interest

The authors declare no conflicts of interest.

References

1. Gupta, A.K.; Wang, T.; Rapaport, J.A. Systematic Review of Exosome Treatment in Hair Restoration: Preliminary Evidence, Safety, and Future Directions. *J. Cosmet. Dermatol.* **2023**, *22*, 2424–2433. [CrossRef]
2. Kost, Y.; Muskat, A.; Mhaimeed, N.; et al. Exosome Therapy in Hair Regeneration: A Literature Review of the Evidence, Challenges, and Future Opportunities. *J. Cosmet. Dermatol.* **2022**, *21*, 3226–3231. [CrossRef]
3. Devjani, S.; Ezemma, O.; Kelley, K.J.; et al. Androgenetic Alopecia: Therapy Update. *Drugs* **2023**, *83*, 701–715. [CrossRef]
4. Gupta, A.K.; Renaud, H.J.; Halaas, Y.; et al. Exosomes: A New Effective Non-Surgical Therapy for Androgenetic Alopecia? *Skinmed* **2020**, *18*, 96–100. [CrossRef]
5. Zhou, Y.; Seo, J.; Tu, S.; et al. Exosomes for Hair Growth and Regeneration. *J. Biosci. Bioeng.* **2024**, *137*, 1–8. [CrossRef]
6. Lee, K.W.A.; Chan, L.K.W.; Hung, L.C.; et al. Clinical Applications of Exosomes: A Critical Review. *Int. J. Mol. Sci.* **2024**, *25*, 7794. [CrossRef]
7. Xiong, M.; Zhang, Q.; Hu, W.; et al. The Novel Mechanisms and Applications of Exosomes in Dermatology and Cutaneous Medical Aesthetics. *Pharmacol. Res.* **2021**, *166*, 105490. [CrossRef]
8. Wang, X.; Xia, J.; Yang, L.; et al. Recent Progress in Exosome Research: Isolation, Characterization and Clinical Applications. *Cancer Gene Ther.* **2023**, *30*, 1051–1065. [CrossRef]
9. Kiselev, A.; Park, S. Immune Niches for Hair Follicle Development and Homeostasis. *Front. Physiol.* **2024**, *15*, 1397067. [CrossRef]
10. Ji, S.; Zhu, Z.; Sun, X.; et al. Functional Hair Follicle Regeneration: An Updated Review. *Signal Transduct. Target. Ther.* **2021**, *6*, 66. [CrossRef]
11. Zhou, L.; Wang, H.; Jing, J.; et al. Regulation of Hair Follicle Development by Exosomes Derived from Dermal Papilla Cells. *Biochem. Biophys. Res. Commun.* **2018**, *500*, 325–332. [CrossRef]
12. Zöller, M.; Zhao, K.; Kutlu, N.N.; et al. Immunoregulatory Effects of Myeloid-Derived Suppressor Cell Exosomes in Mouse Model of Autoimmune Alopecia Areata. *Front. Immunol.* **2018**, *9*, 1279. [CrossRef]
13. Zha, Y.; Li, Y.; Lin, T.; et al. Progenitor Cell-Derived Exosomes Endowed with VEGF Plasmids Enhance Osteogenic Induction and Vascular Remodeling in Large Segmental Bone Defects. *Theranostics* **2021**, *11*, 397. [CrossRef]
14. Kim, H.; Jang, Y.; Kim, E.H.; et al. Potential of Colostrum-Derived Exosomes for Promoting Hair Regeneration Through the Transition from Telogen to Anagen Phase. *Front. Cell Dev. Biol.* **2022**, *10*, 815205. [CrossRef]
15. Li, Y.; Wang, G.; Wang, Q.; et al. Exosomes Secreted from Adipose-Derived Stem Cells Are a Potential Treatment Agent for Immune-Mediated Alopecia. *J. Immunol. Res.* **2022**, *2022*, 7471246. [CrossRef]
16. Wu, J.; Yang, Q.; Wu, S.; et al. Adipose-Derived Stem Cell Exosomes Promoted Hair Regeneration. *Tissue Eng. Regen. Med.* **2021**, *18*, 685–691. [CrossRef]
17. Liang, Y.; Tang, X.; Zhang, X.; et al. Adipose Mesenchymal Stromal Cell-Derived Exosomes Carrying MiR-122-5p Antagonize the Inhibitory Effect of Dihydrotestosterone on Hair Follicles by Targeting the TGF-β1/SMAD3 Signaling Pathway. *Int. J. Mol. Sci.* **2023**, *24*, 5703. [CrossRef]
18. Li, P.; Kaslan, M.; Lee, S.H.; et al. Progress in Exosome Isolation Techniques. *Theranostics* **2017**, *7*, 789. [CrossRef]

19. Heinemann, M.L.; Ilmer, M.; Silva, L.P.; et al. Benchtop Isolation and Characterization of Functional Exosomes by Sequential Filtration. *J. Chromatogr. A* **2014**, *1371*, 125–135. [CrossRef]
20. Chen, B.Y.; Sung, C.W.H.; Chen, C.; et al. Advances in Exosomes Technology. *Clin. Chim. Acta* **2019**, *493*, 14–19. [CrossRef]
21. Ludwig, N.; Whiteside, T.L.; Reichert, T.E. Challenges in Exosome Isolation and Analysis in Health and Disease. *Int. J. Mol. Sci.* **2019**, *20*, 4684. [CrossRef]
22. Hu, S.; Li, Z.; Lutz, H.; et al. Dermal Exosomes Containing miR-218-5p Promote Hair Regeneration by Regulating β-Catenin Signaling. *Sci. Adv.* **2020**, *6*, eaba1685. [CrossRef]
23. Zhang, Y.; Su, J.; Ma, K.; et al. Photobiomodulation Promotes Hair Regeneration in Injured Skin by Enhancing Migration and Exosome Secretion of Dermal Papilla Cells. *Wound Repair Regen.* **2022**, *30*, 245–257. [CrossRef]
24. Rajendran, R.L.; Gangadaran, P.; Bak, S.S.; et al. Extracellular Vesicles Derived from MSCs Activate Dermal Papilla Cell In Vitro and Promote Hair Follicle Conversion from Telogen to Anagen in Mice. *Sci. Rep.* **2017**, *7*, 15560. [CrossRef]
25. Kwack, M.H.; Seo, C.H.; Gangadaran, P.; et al. Exosomes Derived from Human Dermal Papilla Cells Promote Hair Growth in Cultured Human Hair Follicles and Augment the Hair-Inductive Capacity of Cultured Dermal Papilla Spheres. *Exp. Dermatol.* **2019**, *28*, 854–857. [CrossRef]
26. Lee, E.; Choi, M.S.; Cho, B.S.; et al. The Efficacy of Adipose Stem Cell-Derived Exosomes in Hair Regeneration Based on a Preclinical and Clinical Study. *Int. J. Dermatol.* **2024**, *63*, 1212–1220. [CrossRef]
27. Riche, A.; Aberdam, E.; Marchand, L.; et al. Extracellular Vesicles from Activated Dermal Fibroblasts Stimulate Hair Follicle Growth Through Dermal Papilla-Secreted Norrin. *Stem Cells* **2019**, *37*, 1166–1175. [CrossRef]
28. Chen, Y.; Huang, J.; Chen, R.; et al. Sustained Release of Dermal Papilla-Derived Extracellular Vesicles from Injectable Microgel Promotes Hair Growth. *Theranostics* **2020**, *10*, 1454. [CrossRef]
29. Lueangarun, S.; Cho, B.S.; Tempark, T. Rose Stem Cell-Derived Exosomes for Hair Regeneration Enhancement via Noninvasive Electroporation in Androgenetic Alopecia. *J. Cosmet. Dermatol.* **2024**, *23*, 3791. [CrossRef]
30. Lai, J.J.; Chau, Z.L.; Chen, S.Y.; et al. Exosome Processing and Characterization Approaches for Research and Technology Development. *Adv. Sci.* **2022**, *9*, 2103222. [CrossRef]
31. Rahman, E.; Webb, W.R.; Rao, P.; et al. Exosomes Exposed: Overview Systematic Review on Evidence Versus Expectation in Aesthetic and Regenerative Medicine. *Aesthet. Plast. Surg.* **2025**, *49*, 557–568. [CrossRef]
32. Buontempo, M.G.; Alhanshali, L.; Ide, M.; et al. Examining the Uncertainties Surrounding Exosome Therapy in Androgenetic Alopecia: A Call for Evidence-Based Practice. *J. Drugs Dermatol.* **2024**, *23*, e86–e90. [CrossRef]
33. Li, J.; Wang, J.; Chen, Z. Emerging Role of Exosomes in Cancer Therapy: Progress and Challenges. *Mol. Cancer* **2025**, *24*, 13. [CrossRef]